

Dendritic Casting Method as a Novel Crystal Growth Technique to Realize High-quality Si Multicrystals for High-efficiency Solar Cells

In the face of the destruction of the global environment, the degradation of world-wide natural resources and the exhaustion of energy sources in the 21st century, we must establish a sustainable society. Development of high-efficiency solar cells is one of the key technologies to solve the problems of the global environment and energy to aim at sustaining human development and providing high living standards.

In comparison with the traditional energy sources, solar energy is the only ultimate natural energy source. Although ~30% of total solar energy is reflected from the earth surface, the most part of ~70% is utilized by human being. The shipped total power of solar cells in the world rapidly increases in the recent years. The share of the Si multicrystal solar cells is the largest one (~60%) in all types of solar cells. To largely promote the applications of solar cells as an energy source, the present energy cost of the solar cells should be halved. So, the main technology to be developed is the growth method to largely increase the yield of high-quality Si multicrystal ingots, and the growth method to obtain extremely high-quality Si multicrystal ingots.

We have recently developed a reliable method for both purification and structure control to obtain high-quality Si multicrystals with the same grain orientation and large grain sizes by the newly developed dendritic casting method based on deep understanding of crystal growth mechanisms.

To explore the growth mechanism to control microstructures, we newly developed an in-situ observation system to directly observe the growing interface of Si at temperature higher than 1400°C. By utilizing the system, we found that a Si dendrite crystal grew along the bottom of the crucible at the initial stage of the growth followed by the

directional growth on the upper surface of the dendrite crystal under particular growth conditions. Importantly, the upper surface of dendrite crystals can be controlled either {110} or {112} depending on the amount of the supercooling.

This knowledge obtained by the fundamental research lead to develop a novel growth method named as “dendritic casting method” to realize Si multicrystals with the same grain orientation and large grain size. At first, dendrite crystals with the controlled upper plane are grown along the bottom of the crucible under appropriate growth conditions. Subsequently, the growth conditions are controlled to cause directional growth on the upper surface of the dendrite crystals.

By the dendritic casting method, we succeeded in obtaining extremely high-quality Si multicrystal ingots with the same grain orientation and very large grain size as demonstrated by structural analysis and improved conversion efficiency of solar cells. Furthermore, it was found that the conversion efficiency of solar cells is kept high even at the top part of the ingot. This is in contrast with the case for the conventional casting method, where the top part of the ingot is not applicable for solar cells due to segregated impurities. The dendritic casting method is concluded to be promising not only for producing high-quality Si multicrystal ingot but also for increasing yield of high-quality part.

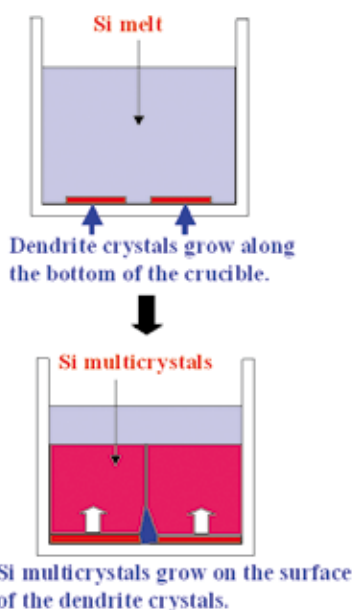


Fig.1 Concept of the dendritic casting method. Dendrite growth along the bottom wall of the crucible is used at the initial stage followed by directional growth.



Fig.2 Outlook of an extremely high-quality Si multicrystal ingot with the same grain orientation and large grain size grown by the dendritic casting method.

References

- [1] K. Fujiwara, W. Pan, N. Usami, K. Sawada, M. Tokairin, Y. Nose, A. Nomura, T. Shishido and K. Nakajima, *Acta Materialia* **54**, 3191 (2006).
- [2] K. Fujiwara, W. Pan, K. Sawada, M. Tokairin, N. Usami, Y. Nose, A. Nomura, T. Shishido and K. Nakajima, *J. Cryst. Growth* **292**, 282 (2006).
- [3] K. Fujiwara, Y. Obinata, T. Ujihara, N. Usami, G. Sazaki and K. Nakajima, *J. Cryst. Growth* **262**, 124 (2004).

Contact to

Kazuo Nakajima (Crystal Physics Division)
e-mail: nakasisc@imr.tohoku.ac.jp

High Brightness Light Emitting Diodes by Metal buffer and Chemical Lift-Off Techniques

Device quality GaN layers and LEDs (Light Emitting Diodes) were successfully grown on sapphire substrate with metal buffer layers. GaN layers and LED structure were separated from sapphire substrate by chemically selective etching of metal buffer layer. This chemical lift-off (CLO) process is easily transferred to the vertical LED process and very powerful for mass-production. CLO processes should also be applicable and suitable for high-power and large-area LEDs.

Recently, III-nitrides have promoted great advances in LEDs. High efficiency GaN-based LEDs attract great interest for applications such as displays, traffic signals, back light for Liquid crystal display (LCD) and white-light sources. However, the total light output from these LEDs is still rather low. Many approaches have been carried out to increase the external efficiency, including roughening the surface of LEDs, p-side down LEDs, patterned substrate, photonic crystal LEDs, reflective metals and flip-chip techniques. Kelly et al. first demonstrated the laser lift-off (LLO) technique to separate a HVPE grown GaN layer from sapphire. The LLO technique has been used to fabricate the vertical type GaN/InGaN LEDs. The luminance intensity is over two times stronger than that of the original planar GaN/sapphire LED. However, the LLO technique has some problems; 1) complicated process, 2) not suitable for mass production, 3) high expensive laser system, 4) formation of micro cracks on de-bonding and 5) lift-off side damage by laser.

We succeed in growing high crystallinity GaN by inserting metal buffer layers between sapphire substrates and GaN epitaxial layers. GaN layers and LED structure were separated from sapphire substrate by chemically selective etching of metal buffer layer, i.e. CLO process. The development of metal buffer layers and chemical lift-off process can supply new process for high brightness vertical LEDs, which results in low cost process and strong impacts on optical and electronic device structure. Figure 1 shows the CLO process flow for fabrication of vertical LEDs.

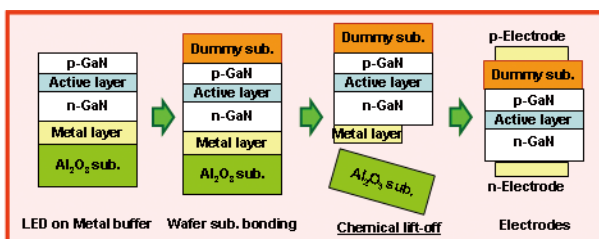


Fig.1. CLO processes for fabrication of vertical LED

The CLO technique has advantages of damage-free and simple process. Hence, the V-LEDs manufactured by CLO processes have a high-efficient and reliable characteristic for high-brightness LED applications, such as backlights for flat panel display in LCD, automotive headlights and general room lightings.

Based on GaN growth on metal buffer and CLO technique, we fabricated vertical LEDs as shown in fig. 2.

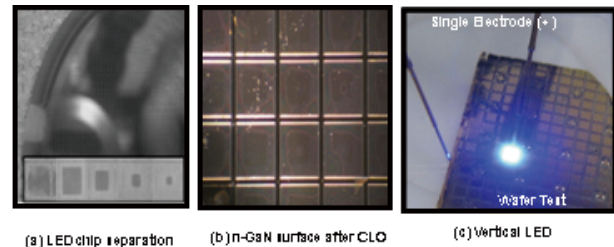


Fig.2. (a) Selective metal buffer etching. (b) n-GaN surface separated from sapphire by CLO process. (c) vertical LEDs.

Fig. 2(a) is a picture of a laser scribed GaN wafer grown on metal buffer, the bottom images show etching progress of a chip. The metal buffer layer is being etched out by etchant as time goes. The impact of this achievement is that any post processes such as lapping, polishing are not needed any more for device manufacturing, if the CLO process is applied. Fig. 2 (b) shows an n-GaN back surface of a LED structure separated from sapphire after CLO process. The surface shows very smooth morphology without any cracks. Fig. 2 (c) shows surface emission of a V-LED with top-down electrodes.

The crystalline quality of GaN layers grown on sapphire with metal buffer is even better than those grown with low temperature GaN or AlN buffer layers. Hence, both high operation current and substantial improvement in light output power can be realized with CLO process. Based on the present achievements, the CLO process is applicable and suitable for the fabrication of high-power and large-area LEDs. It offers simpler processes for mass production of V-LEDs, which should lead to cost-down of V-LEDs, in turn should drive solid-state lighting in the world.

References

- [1] S. W. Lee, D. C. Oh, H. Goto, J. S. Ha, H. J. Lee, T. Hanada, M. W. Cho, S. K. Hong, H. Y. Lee, S. R. Cho, J. W. Choi, J. H. Choi, J. H. Jang, J. E. Shin, J. S. Lee and T. Yao, Phys. stat. sol. (c) 4, 37 (2007)
- [2] S. W. Lee, D. C. Oh, H. Goto, J. S. Ha, H. J. Lee, T. Hanada, M. W. Cho, T. Yao, S. K. Hong, H. Y. Lee, S. R. Cho, J. W. Choi, J. H. Choi, J. H. Jang, J. E. Shin, Appl. Phys. Lett. 89, 132117 (2006)
- [3] W. H. Lee, S. W. Lee, H. Goto, H. C. Ko, M. W. Cho, T. Yao, Phys. stat. sol. (c) 3, 1388 (2006)

Contact to

Takafumi Yao (Physics of Electronic Materials Division)
e-mail: yao@cir.tohoku.ac.jp

How is Crystal Growth Affected by an External Electric Field?

A nanoscopic approach was applied to bulk crystal growth by sustaining a large electric field in the electric double layer induced by an external electric field. This affected the phase equilibria and growth dynamics and represents a new approach to crystal growth.

Bulk crystals are frequently grown by the conventional Czochralski or Bridgman method, in which the temperature gradient, pulling rate, and rotation rate, etc. are the only parameters that can be optimized for producing “high-quality” crystals. Researchers have been elaborating these parameters on crystal growth in systems that are normally constrained by two variables; “composition” and “temperature” at a fixed pressure. In order to unbind the restriction of the limited freedom of “composition” and “pressure”, we have introduced a third parameter, namely an external electric field, to add an additional degree of freedom to crystal growth.

Figure 1 shows that the relationship between the energies of the solid and the melt is critical for improving crystal growth. One should consider phase equilibria in the case when there is no energy difference, and growth dynamics in which the energy difference is a driving force for nucleation and growth. Applying an external electric field to the growth system alters both the phase equilibria and growth dynamics, which has the potential to lead to a new crystal growth mechanism. We have demonstrated the conversion of the melting state of langasite ($\text{La}_3\text{Ga}_5\text{SiO}_{14}$) from incongruent to congruent [1] by the imposition of an electric field as large as 10^4 V/cm which is sustained in the electric double layer between a platinum crucible wall and langasite melt [2]. This is a good news for reviving many incongruent-melting materials which are difficult to grow and thus have been unused even though they have superior functional properties.

Concerning the effect of an applied electric field on growth

dynamics, we have demonstrated that the dissolution of the 211 phase into solution was greatly enhanced by applying an electric field in the case of the peritectic reaction of the 211 phase with a solution to form YBCO (123 phase) [3]. This change occurred at the growth front and is attributed to a 20% reduction in the activation energy for dissolution (Fig. 2).

It should be noted that these modifications of crystal growth by an applied electric field occurred in an ultra-thin layer having a thickness of the order of nanometers, the so-called “electric double layer”. Because the oxide melt is electrically conductive due to the presence of ionic species in it, an external applied field does not penetrate into the bulk melt, but rather it generates a very large electric field in the electrical double layer. This phenomenon is interesting since it demonstrates that macroscopic operation can lead to nanoscopic control. This study could be said to be the first attempt of performing bulk crystal growth in a nanoscopic manner.

References

- [1] S. Uda, X. Huang and S. Koh, *J. Cryst. Growth* **281**, 481 (2005).
- [2] S. Uda, S. Koh and X. Huang, *J. Cryst. Growth* **292**, 1 (2006).
- [3] X. Huang, S. Uda, X. Yao and S. Koh, *J. Cryst. Growth* **294**, 420 (2006).

Contact to

Satoshi Uda (Crystal Chemistry Division)

e-mail: uda@imr.tohoku.ac.jp

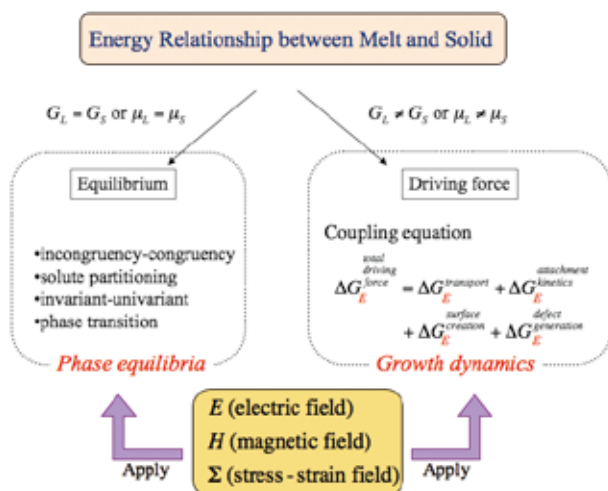


Fig. 1 Relationship between the energies of the solid and melt in association with phase equilibria and growth dynamics. An external electric field significantly modifies this relationship, and so represents a new fresh approach to crystal growth.

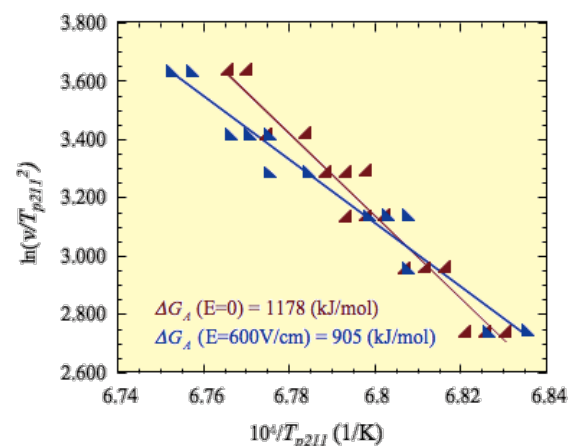


Fig. 2 Relationship between $\ln(v/T_{p211}^2)$ and $1/T_{p211}$ for investigating the activation energy of dissolution of 211.

Materials Designing of Metal Borohydrides as Advanced Hydrogen Storage Materials

Systematic research and development on borohydrides, promising candidates as high-density hydrogen storage materials, were performed from experimental and theoretical viewpoints.

Some types of borohydrides such as LiBH_4 , $\text{Mg}(\text{BH}_4)_2$, and $\text{Ca}(\text{BH}_4)_2$ [1, 2] have attracted considerable attention as high-density hydrogen storage materials, especially for fuel cell applications. Crystal structure of LiBH_4 is shown in Fig. 1.

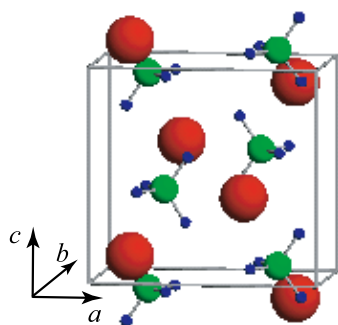


Fig. 1 Crystal structure of low-temperature phase of LiBH_4 . $a = 0.718$ nm, $b = 0.444$ nm, and $c = 0.680$ nm (space group: Pnma (#62)). Red (large), green (middle), and blue (small) spheres represent Li, B, and H atoms, respectively.

We investigated thermodynamical stabilities of a series of alkali-, alkaline-earth-, and transition-metals borohydrides ($M(\text{BH}_4)_n$ with $M = \text{Li}, \text{Na}, \text{Mg}, \text{Sc}, \text{Zn},$ and Zr ; $n = 1\text{--}4$) by using both the first-principles studies and hydrogen desorption measurements [1]. The theoretical study indicated that the charge transfer from cation M^{n+} to complex anion $[\text{BH}_4]^-$ is a key feature for the stability of $M(\text{BH}_4)_n$, and also that there exists a linear relationship between calculated heat of formation ΔH_{form} of $M(\text{BH}_4)_n$ and Pauling electronegativity χ_P of M . Experimentally, $M(\text{BH}_4)_n$ was successfully synthesized on the basis of the following solid-state metathesis (SSM) reaction:

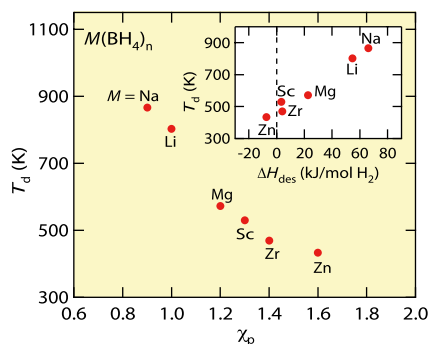


Fig. 2 Hydrogen desorption temperature T_d of $M(\text{BH}_4)_n$ as a function of Pauling electronegativity χ_P of M . Inset shows the correlation between T_d and estimated enthalpy change of hydrogen desorption reaction ΔH_{des} .

Hydrogen desorption temperature T_d of $M(\text{BH}_4)_n$ determined using gas-chromatography was also closely correlated with χ_P , as shown in Fig. 2. T_d decreases with an increase in the value of χ_P . Therefore, we conclude that the value of χ_P is a useful indicator that assists in the estimation of the thermodynamical stabilities of “single-cation” borohydrides $M(\text{BH}_4)_n$ with the corresponding value of T_d in various temperature ranges.

Thermodynamical stabilities of “multi-cation” borohydrides $MM'(\text{BH}_4)_n$ were also investigated. For example, hydrogen desorption temperature T_d of $\text{ZrLi}_{n-4}(\text{BH}_4)_n$ ($n = 4, 5,$ and 6) increases from 440 K to 650 K as the value of composition n increases, and continuously approaches toward 740 K — T_d of LiBH_4 . Thus, the correlation between T_d and χ_P observed in “single-cation” borohydrides can be reasonably extended to “multi-cation” ones; T_d correlates with the averaged value of χ_P calculated from n .

In addition to the materials designing of borohydrides $M(\text{BH}_4)_n$ focusing on electronegativity of M , formation of intermediate compounds are found to be of great importance to promote their hydrogen desorption reaction [3, 4]. For example, LiBH_4 starts to change into an intermediate compound at the temperature range over 700 K, accompanying the partial hydrogen desorption reaction. Although the compound does not show long-range ordering for the powder X-ray diffraction measurement, the local atomistic structure can be investigated by the laser Raman spectroscopy; the B-H bending modes have lower frequencies as compared to those of LiBH_4 , while the B-H stretching modes appear at higher frequencies [3]. These features are fairly consistent with the theoretical calculation on the monoclinic $\text{Li}_2\text{B}_{12}\text{H}_{12}$, consisting of Li^+ and $[\text{B}_{12}\text{H}_{12}]^{2-}$ ions, as a possible intermediate compound of LiBH_4 [4]. The further experimental studies on the atomistic and electronic structures of the compound, and also on hydrogen desorption and re-adsorption reactions of LiBH_4 using appropriate intermediate compounds are now in progress.

Neutronics assessment as advanced neutron shield materials for fusion reactors [5], and combination research between hydrogen storage and microwave technologies [6] were also successively carried out using the series of borohydrides.

References

- [1] Y. Nakamori et al., *Phys. Rev. B* **74**, 045126 (2006).
- [2] K. Miwa et al., *Phys. Rev. B* **74**, 155122 (2006).
- [3] S. Orimo et al., *Appl. Phys. Lett.* **89**, 021920 (2006).
- [4] N. Ohba et al., *Phys. Rev. B* **74**, 075110 (2006).
- [5] T. Hayashi et al., *Fusion Eng. Design* **81**, 1285-1290 (2006)
- [6] Y. Nakamori et al., *Appl. Phys. Lett.* **88**, 112104 (2006).

Contact to

Shin-ichi Orimo (High-Temperature Materials Science (Environmental Materials Science) Division)
e-mail: orimo@imr.tohoku.ac.jp

Two-dimensional Images of Emission Spectra from Laser Induced Plasmas and the Application to Emission Spectrometric Analysis

Spatial distribution analysis of emission signals from a laser-induced plasma can provide information on the optimization of the analytical conditions when it is employed as a sampling and excitation source in optical emission spectrometry. A two-dimensionally imaging spectrometer system is employed to measure the spatial variations in the emission intensities of analytes.

Laser-induced plasma spectrometry (LIPS) is a powerful technique for direct analysis of various materials because of the rapid response without any sample pre-treatment. A Q-switched Nd:YAG laser, which is irradiated onto a sample surface during a very short period but with a large power density, produces a pulsed laser-induced plasma (LIP) at the repetition frequency of the laser. Sample atoms are ejected from the surface due to laser ablation and are subsequently ionized and excited in LIP; therefore, this plasma acts as an excitation source as well as a sampling source for atomic emission spectrometry.

The LIP has both spatial and temporal variations depending on various experimental parameters, such as the kind and the pressure of the plasma gas, which is generally called an expansion of the plasma plume. Previous papers reported that the emission zone varied with the progress of the plasma plume, which was strongly dependent on the nature of the plasma gas. It is further known that LIPs produced at reduced pressures have favorable features for emission analysis because of the relatively low fluctuation of the emission intensities as well as the large signal-to-background ratio. Time-resolved measurement of the emission spectra thus gives useful information on optimization of the experimental conditions in the emission spectrometric applications, such as the delay time as well as the exposure time on the data acquisition [1,2]; however, it cannot provide the overall variations of the plasma expansion. For this purpose, the two-dimensional (2D) image of a spectral line emitted from the LIP should be observed, which is expected to yield information on the fundamental processes occurring in the LIP. However, few studies have been published mainly due to lack of spectrometers enabling 2D observation having good spectral resolution.

In this study, we investigate 2D images of emission lines of copper from a reduced-pressure LIP when krypton, argon, or helium is employed as the plasma gas and their variations against the gas pressures in order to discuss the excitation mechanism for each plasma gas.

A schematic diagram of the apparatus is shown in Fig. 1. A Nd:YAG laser (LOTIS T II U LS-2135, Japan) was employed at the wavelength of 532 nm (SHG mode). The laser energy of 40 mJ/pulse was set to obtain sufficient sample ablation. The pulse duration of about 10 ns and the repetition rate of 10 Hz were employed. A spherical lens with a 200-nm focal length was used to focus the laser beam onto the target surface. High-purity copper plates (99.99%) were used as the sample. High-purity argon (>99.9999%), krypton (>99.999 %), and helium (>99.99999 %) were introduced as the plasma gas after evacuation of the chamber below 7 Pa. On keeping 2D spatial information, emission signals from the LIP were conducted through a telescope optics onto the entrance slit of an image spectrometer (Model 12580, BunkoKeiki Corp., Japan), and the emission image is then dispersed and detected on a charge-coupled device detector (SensiCam QE Model, PCO Imaging Corp., Germany). The spectral resolution was 0.1-0.5 nm depending on the slit width. The plasma images were recorded for the period of 0.01 ms (gate width).

Figure 1 shows 2D emission images of the Cu I 324.75 nm and the background at 315.0 nm when argon gas was introduced at various pressures [3]. It is found from these coloured maps that the intensities

are larger at higher gas pressures and that the images roughly comprise two portions: a narrow spot near the sample surface occurring the breakdown of LIP and a portion expanding towards the surrounding gas which is called a plasma plume. The shape and the intensities of the emission zone are considered to be determined through the interaction between energetic particles produced immediately after the laser breakdown and the surrounding gas. In this case, the copper emission from the plasma plume should be measured for emission analysis due to the small background level, compared to the breakdown position. It is expected that the 2D imaging of LIP can yield an optimum condition regarding the plasma portion observed when it is employed for the analytical application.

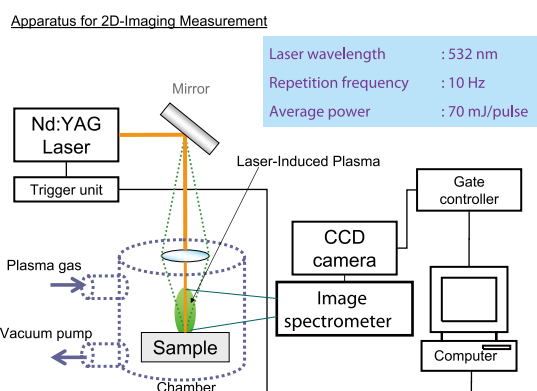


Fig 1. Experimental setup for 2D-imaging measurement.

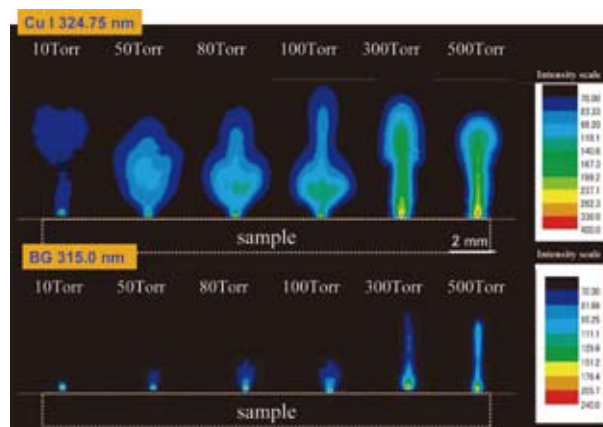


Fig 2. Two-dimensional images of laser-induced plasmas measured at Cu I 324.75 nm and BG 315.0 nm at various argon pressures of 10, 50, 80, 100, 300, and 500 Torr.

References

- [1] Y. Ushirozawa and K. Wagatsuma, *Spectrosc. Lett.* **28**, 539 (2005).
- [2] Y. Ushirozawa and K. Wagatsuma, *Anal. Sci.* **22**, 1011 (2006).
- [3] C. Kitaoka and K. Wagatsuma, *Proc. of 12th International Symposium on Advanced Technology and Applications*, 72 (2006).

Contact to

Kazuaki Wagatsuma (Analytical Science Division)
e-mail: kwagatsuma@mm.newweb.ne.jp

Improvements of Superconducting Properties for Practical Nb₃Sn Wires by the Mechanical Treatment

It is well known that practical Nb₃Sn superconducting wires are deteriorated by the residual strain, because of their large strain sensitivity. We found that the mechanical treatment at room temperature improves the superconducting performance drastically. This new but simple technique can control and optimize the residual strain state and is effective the improvement of the strain dependence of the superconducting parameters

Nb₃Sn superconducting wires are now utilized widely for most superconducting power devices with high magnetic fields above 10 T. Generally the superconducting wires have a composite architecture of the fine Nb₃Sn filaments with Cu, Nb/Ta and sometime high strength materials as shown in Fig.1, from the requirement of a formation of Nb₃Sn phase, a stability of the superconductivity, a diffusion barrier and a reinforcement. However, it is well known that some unsolved problems such as a non-stoichiometry, residual strain and mechanical properties are still remained. Hence it is expected that the superconducting performance of the practical Nb₃Sn wires would be improved drastically, if those problems can be solved. We have already developed the high strength Nb₃Sn wire reinforced by the Cu-based micro-composite materials such as CuNb [1]. Figure 1 represents the cross-sectional view of the typical high strength Nb₃Sn wire developed by our group. Due to the reinforcement, the stress dependence of critical current density J_c is improved by about twice of the stress due to the reinforcement in comparison with the conventional Nb₃Sn wires (blue triangle) as shown in Fig. 2 (b). In other words, the high strength Nb₃Sn wires can be utilized in high stress states up to 250-300 MPa. However, the residual strain induced by the thermal contraction difference between Nb₃Sn and materials composing the wire still deteriorates the superconducting parameters, i.e., a critical current density, an upper critical field and a critical temperature, when the wires are cooled from the heat treatment temperature to 4.2 K. When the axial tensile stress is given to the Nb₃Sn wires, the J_c values usually increase first and become the maximum at the certain stress/strain as shown in Fig.2 (b). This stress/strain at the maximum J_c corresponds to the thermal residual stress/strain.

Recently, we found that the mechanical treatment of the repeated bending at room temperature enhances J_c as

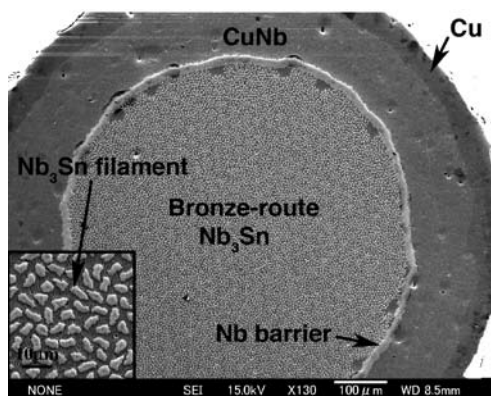


Fig. 1 Cross-section of the typical high strength Nb₃Sn wire.

shown in Fig. 2(a). For example the J_c value becomes twice after the repeated bending. We call this phenomenon “prebending” effect. Due to the prebending treatment, the strain dependence of J_c shifts to lower strain and the maximum J_c value also increases at the same time as shown in Fig. 2(b). This suggests that the reduction of not only the axial residual strain but also the radial one due to the prebending treatment. We successfully confirmed the change of the 3-dimensional strain states directly by the neutron diffraction at the first in the world [3]. Finally, we got high performance of J_c in the wide stress region as shown in Fig.2 (b) by both of the high-strength and the prebending treatment. In addition, the prebending effect would be a key technique to clarify the strain dependence of J_c for the strain sensitive superconducting materials.

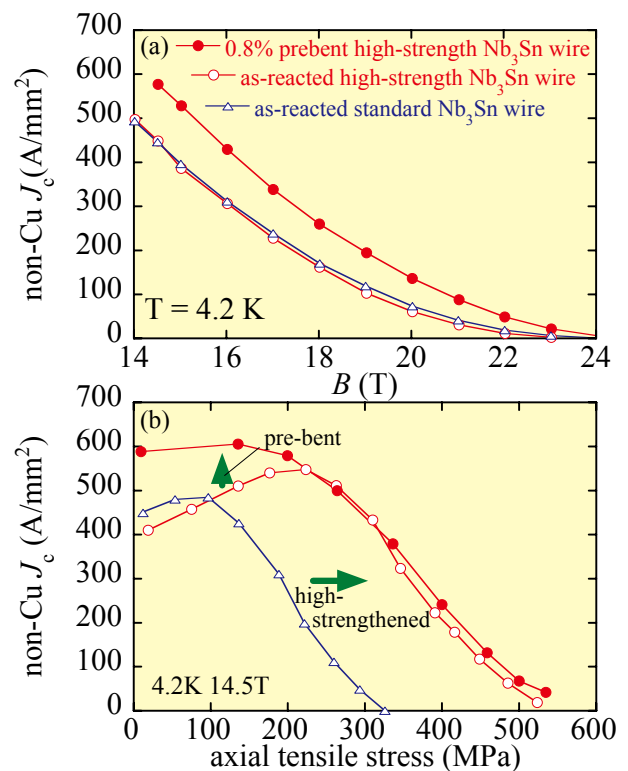


Fig. 2 (a) Field dependence and (b) axial stress dependence of J_c for the standard Nb₃Sn without reinforcement and the high-strength Nb₃Sn wires with and without prebending.

References

- [1] K. Watanabe, S. Awaji, K. Katagiri, K. Noto, K. Goto, M. Sugimoto, T. Saito, and O. Kohno, IEEE Trans. Magn. **30**, 1871 (1994).
- [2] S. Awaji, K. Watanabe, H. Oguro, G. Nishijima, T. Tsubouchi, K. Miyoshi, S. Meguro, Fusion Eng. Design **81**, 2473 (2006).
- [3] H. Oguro, S. Awaji, G. Nishijima, P. Badica, K. Watanabe, F. Shikanai, T. Kamiyama, K. Katagiri, J. Appl. Phys. **101**, 103913 (2007).

Contact to

Satoshi Awaji (High Field Lab. for Superconducting Materials)
e-mail: awaji@imr.tohoku.ac.jp